Author's personal copy

Microbial Pathogenesis 51 (2011) 225-229



Contents lists available at ScienceDirect

Microbial Pathogenesis

journal homepage: www.elsevier.com/locate/micpath



Short Communication

Subcellular localizations and time-course expression of dengue envelope and non-structural 1 proteins in human endothelial cells

Jesdaporn Poungsawai a,b, Rattiyaporn Kanlaya a, Sa-nga Pattanakitsakul c, Visith Thongboonkerd a,d,*

- a Medical Proteomics Unit, Office for Research and Development, Faculty of Medicine Siriraj Hospital, Mahidol University, Bangkok, Thailand
- b Department of Immunology and Immunology Graduate Program, Faculty of Medicine Siriraj Hospital, Mahidol University, Bangkok, Thailand
- ^c Medical Molecular Biology Unit, Office for Research and Development, Faculty of Medicine Siriraj Hospital, Mahidol University, Bangkok, Thailand
- ^d Center for Research in Complex Systems Science, Mahidol University, Bangkok, Thailand

ARTICLE INFO

Article history: Received 22 July 2010 Received in revised form 23 April 2011 Accepted 29 April 2011 Available online 7 May 2011

Dengue Endothelial cells Envelope NS1 Subcellular localization Viral proteins

Keywords:

ABSTRACT

We performed subcellular fractionation of human endothelial cells (EA.hy926) after a challenge with dengue virus serotype-2 (DEN-2) at multiplicity of infection (MOI) of 10 for 2 h. The cells were fractionated into four fractions including cytosol, membrane/organelle, nucleus and cytoskeleton, and their purity was nicely confirmed by immunofluorescence staining of markers for individual subcellular compartments. Western blot analysis of dengue envelope (E) and non-structural 1 (NS1) proteins showed that E was present only in membrane/organelle fraction, whereas NS1 was present in membrane/organelle, nucleus, and cytoskeleton fractions. Time-course study showed that E was present immediately after the challenge, whereas NS1 was present after 12 h of the challenge. Our data may provide a new roadmap for studying mechanisms of replication of dengue virus and its interactions with host cells.

© 2011 Elsevier Ltd. All rights reserved.

1. Introduction

Dengue virus infection remains an important public health problem worldwide, particularly in tropical and sub-tropical areas [1]. The severe forms of dengue virus infection include dengue hemorrhagic fever (DHF) and dengue shock syndrome (DSS), of which pathogenic mechanisms are still unclear. Like other flaviviruses, dengue virus enters into target cells through receptormediated endocytosis using glycosylated envelope (E) protein as a binding ligand to particular receptor(s) [2,3]. After endocytosis, low pH milieu of the endosome triggers E protein to undergo conformational change, exposing a hydrophobic fusion peptide that initiates fusion of virus-host membrane lipid bilayers [4]. The

Abbreviations: BSA, bovine serum albumin; DEN-2, dengue virus serotype-2; E, envelope protein; ER, endoplasmic reticulum; FBS, fetal bovine serum; hnRNP C1/C2, heterogeneous nuclear ribonucleoprotein C1/C2; MOI, multiplicity of infection; NS1, non-structural 1 protein; RT, room temperature.

E-mail addresses: (V. Thongboonkerd).

thongboonkerd@dr.com,

vthongbo@yahoo.com

fusion step is crucial for releasing the viral genome to allow successful viral replication in the cytoplasm. Since the genome of dengue virus is a positive-sense RNA strand, the single open reading frame of genome can be translated into single polyprotein, which subsequently undergoes post-translational modification(s) by viral and host proteases. This important step generates three structural proteins including capsid, pre-membrane and E proteins, and seven non-structural (NS) proteins including NS1, NS2A, NS2B, NS3, NS4A, NS4B and NS5. These NS proteins are involved in viral replication, protease activity and RNA polymerase activity. Most of these NS proteins are not packed into viral particles but play important role in viral replication [5].

Generally, RNA viruses do not require any association with the nucleus to induce their replication process. Nevertheless, several lines of evidence have demonstrated the interaction of some RNA viruses with the nuclei of host cells to facilitate viral replication [6,7]. Picornaviruses are the good examples for this association. Through the virus—nucleus interaction, the RNA viruses relocate some nuclear factors regulating transcription of host cell defenses to escape from immunity as well as recruit them to benefit their replication inside the cytoplasm [7]. Some viral proteins, particularly viral proteases, target to the nucleus with their precursor forms containing nuclear localization signal (NLS) to interfere the

^{*} Corresponding author. Medical Proteomics Unit, Director of Center for Research in Complex Systems Science (CRCSS), Siriraj Hospital, Mahidol University, 12th Floor Adulyadej Vikrom Building, 2 Prannok Road, Bangkoknoi, Bangkok 10700, Thailand. Tel./fax: +66 2 4184793.

host transcription process by degrading the cellular transcription machinery [7]. In the case of flaviviruses, active RNA-dependent viral polymerases, including NS3 and NS5, have been found within the nuclei of the cells infected with West Nile virus, Japanese encephalitis virus, and dengue virus [8]. These findings suggest that host cell nucleus also serves as an additional site for active flaviviral replication [8].

Even with the aforementioned information, molecular mechanisms underlying dengue virus replication in the target host cells remain unclear. To better understand such mechanisms, the information of subcellular localizations and time-course expression of viral proteins in infected cells, which are the major targets for dengue virus infection, is crucial. However, such information was under-investigated in previous studies. Therefore, the present study was conducted to obtain such information using subcellular fractionation (based on stepwise extraction by various lysis buffers), Western blot analysis, and immunofluorescence staining.

2. Results & discussion

After 24-h of the challenge with DEN-2 at MOI of 10 for 2 h, the condition of which infectivity was approximately 90% without significant increase of cell death as described in our previous study [9], the cell monolayer was subjected to subcellular fractionation using ProteoExtract Subcellular Proteome Extraction Kit (Mini sPEK). Basically, this kit fractionated subcellular compartments by stepwise extraction using different extraction buffers, of which potency/capacity to solubilize proteins differed (Fig. 1A). Compositions of individual buffers used for differential extraction are provided as Supporting Information. Using this kit, the DEN-2-infected cells were successfully fractionated into four fractions, including cytosol (F1), membrane/organelle (F2), nucleus (F3) and cytoskeleton (F4).

The purity of all these fractions was examined by immunofluorescence staining of markers for individual subcellular

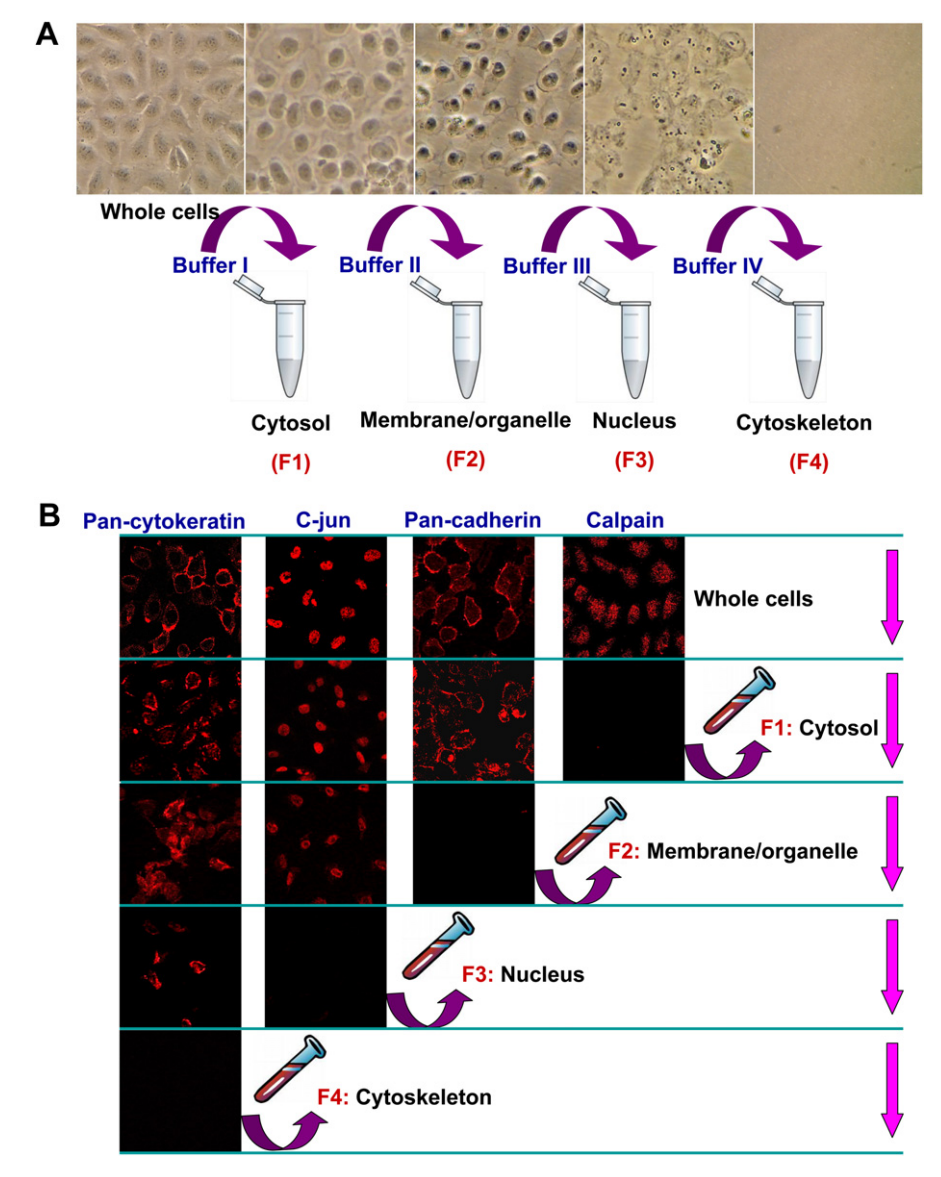


Fig. 1. Subcellular fractionation and its purity. Panel (A) shows schematic summary of basic methods used for subcellular fractionation, based on stepwise extraction by differential buffers of which potency to solubilize proteins differed. Panel (B) demonstrates the purity of subcellular fractionation. Top panels show immunofluorescence staining patterns of markers for cytosol (calpain), membrane/organelle (pan-cadherin), nucleus (c-jun), and cytoskeleton (pan-cytokeratin). After collecting each subcellular fraction, the corresponding marker was absent, whereas the markers for other remaining fractions were still present. Original magnification power was 630X for all panels.

compartments. Fig. 1B shows that our fractionation steps yielded highly purified subcellular fractions. Western blot analysis revealed that E protein was present only in membrane/organelle fraction (Fig. 2A), whereas NS1 protein was present in membrane/organelle, nucleus, and cytoskeleton fractions (most prominent in membrane/organelle fraction) (Fig. 2B).

Our results suggested that these dengue proteins may be associated with intracellular organelles, which were used as the cargo for protein translation and/or viral replication. Indeed, this is not surprising as translation and replication of positive-strand viruses, especially dengue virus, have been thought to localize in intracellular membrane structures or endoplasmic reticulum (ER)-associated membranes [10]. E protein is a part of (endosomal) membrane that binds with pre-membrane protein to form a heterodimer for viral assembly during maturation. Therefore, it is reasonable that E protein was identified in the membrane/organelle fraction (Fig. 2A).

NS1 protein has been identified as many different forms; i.e., ERassociated replication complex, membrane-anchored form, and secreted form [11-13]. Our present study identified NS1 at approximately 80 kDa, which was most likely its dimer form. Indeed, newly synthesized NS1 is transiently expressed as a monomer but rapidly forms a homodimer in the ER [14]. The homodimeric NS1 becomes partially hydrophobic and is associated with cellular membranes [12]. Our data showed that NS1 was present predominately in the membrane/organelle fraction, consistent with the findings on characteristics and functional roles of NS1 reported in many previous studies. However, it is surprising to find NS1 in the nucleus and cytoskeleton fractions. This novel finding could be explained by the findings reported in a previous study demonstrating that NS1 interacts with heterogeneous nuclear ribonucleoprotein isoform C1/C2 (hnRNP C1/C2) [15]. Moreover, our recent study clearly demonstrated that NS1 also interacts with vimentin, a cytoskeletal protein that plays significant role in dengue virus replication [16].

We then performed serial analysis of double-immunofluorescence staining of dengue protein (E or NS1) and host pan-cadherin protein (a marker for membrane/organelle) to demonstrate time-course expression of dengue E and NS1 proteins, and to confirm their localization in membrane/organelle compartment. Dengue E protein was observed as early as 0 h after the challenge with DEN-2 (at MOI of 10 for 2 h) (Fig. 3A), whereas NS1 was detectable after 12 h of DEN-2 challenge (Fig. 3B). The

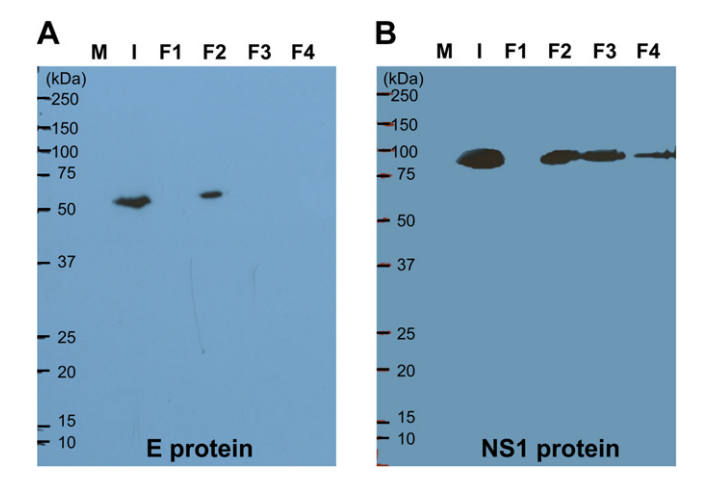


Fig. 2. Western blot analysis of DEN-2 envelope (E) and non-structural 1 (NS1) proteins (panels (A) and (B), respectively). DEN-2-infected EA.hy926 cells (at 24-h after the challenge with DEN-2 at MOI of 10 for 2 h) were fractionated into 4 subcellular fractions, including cytosol (F1), membrane/organelle (F2), nucleus (F3) and cytoskeleton (F4). M and I denote whole cell lysates of mock-control and DEN-2-infected cells, respectively, and served as negative and positive controls, respectively.

intensity of staining was progressively increased when the postchallenge incubation time was prolonged, indicating viral replication. The earlier detection of dengue E protein might be due to its earlier translation based on its locus in the genome or the differential sensitivity of antibody used. We also observed co-localization of both dengue proteins with pan-cadherin (Fig. 3C and D), consistent with the data presented in Fig. 2 demonstrating that E and NS1 were localized predominately in membrane/organelle fraction. Indeed, Fig. 3C and D were derived from 24-h postchallenge time-point, which was the identical condition used in Western blot analysis shown in Fig. 2. However, the co-localization of dengue proteins and pan-cadherin was better illustrated at earlier time-points, which provided a clearer membrane and granular pattern of pan-cadherin, whereas this pattern was flared by overwhelming abundance levels of E and NS1 at 24-h timepoint. Interestingly, we did not observe intra-nuclear expression of NS1 protein by immunofluorescence staining, whereas Western blot data clearly demonstrates the expression of NS1 in the nucleus fraction. Whereas there was no doubt on the purity of our subcellular fractionation steps (see Fig. 1B), this contradictory results could be explained that NS1 protein is also expressed at perinuclear, but not intra-nuclear, region to interact with hnRNP C1/ C2, which can be shuttled between nucleus and other cellular compartments [17,18].

In summary, we report herein for the first time subcellular localizations and time-course expression of dengue E and NS1 proteins in human endothelial cells. Our data also demonstrate the strength of fractionation method, which provided highly purified subcellular compartments, and thus is the useful technique for studying mechanisms of viral replication and related intracellular processes. Our data may also offer opportunities to further explore interactions between dengue virus and host cellular proteins, which are involved in viral replication, maturation and assembly.

3. Materials & methods

3.1. Cell cultivation and dengue virus infection

Human endothelial cells (EA.hy926) were cultured in Dulbecco's minimum essential medium/F-12 (DMEM/F-12) (GIBCO; Grand Island, NY) supplemented with 10% heat-inactivated fetal bovine serum (FBS) (GIBCO), 100 U/ml penicillin G and 100 mg/ml streptomycin (SIGMA; St. Louis, MO). The cells were then challenged with dengue virus serotype-2 (DEN-2) (strain 16681) at the multiplicity of infection (MOI) of 10 for 2 h at 37 °C.

3.2. Subcellular fractionation

After 24-h of the challenge with DEN-2, the cell monolayer was subjected to subcellular fractionation using ProteoExtract Subcellular Proteome Extraction Kit (Mini sPEK) (Calbiochem, EMD Biosciences; Darmstadt, Germany) according to the manufacturer's instruction. Buffer I (pH 6.8) contained 10 mM PIPES, 0.02% digitonin, 300 mM sucrose, 15 mM NaCl, and 0.5 mM EDTA; Buffer II (pH 7.4) contained 10 mM PIPES, 0.5% triton X-100, 300 mM sucrose, 15 mM NaCl, and 0.5 mM EDTA; Buffer III (pH 7.4) contained 10 mM PIPES, 1.0% tween-40, 0.5% deoxycholate, 350 mM NaCl, and 500 U/ml benzonase; and Buffer IV (pH 7.4) contained 5% SDS, 10 mM Na₂HPO₄, and 10 mM H₂PO₄.

3.3. Immunofluorescence staining of markers for individual subcellular compartments

The purity of all subcellular fractions was examined by immunofluorescence staining of markers for individual subcellular

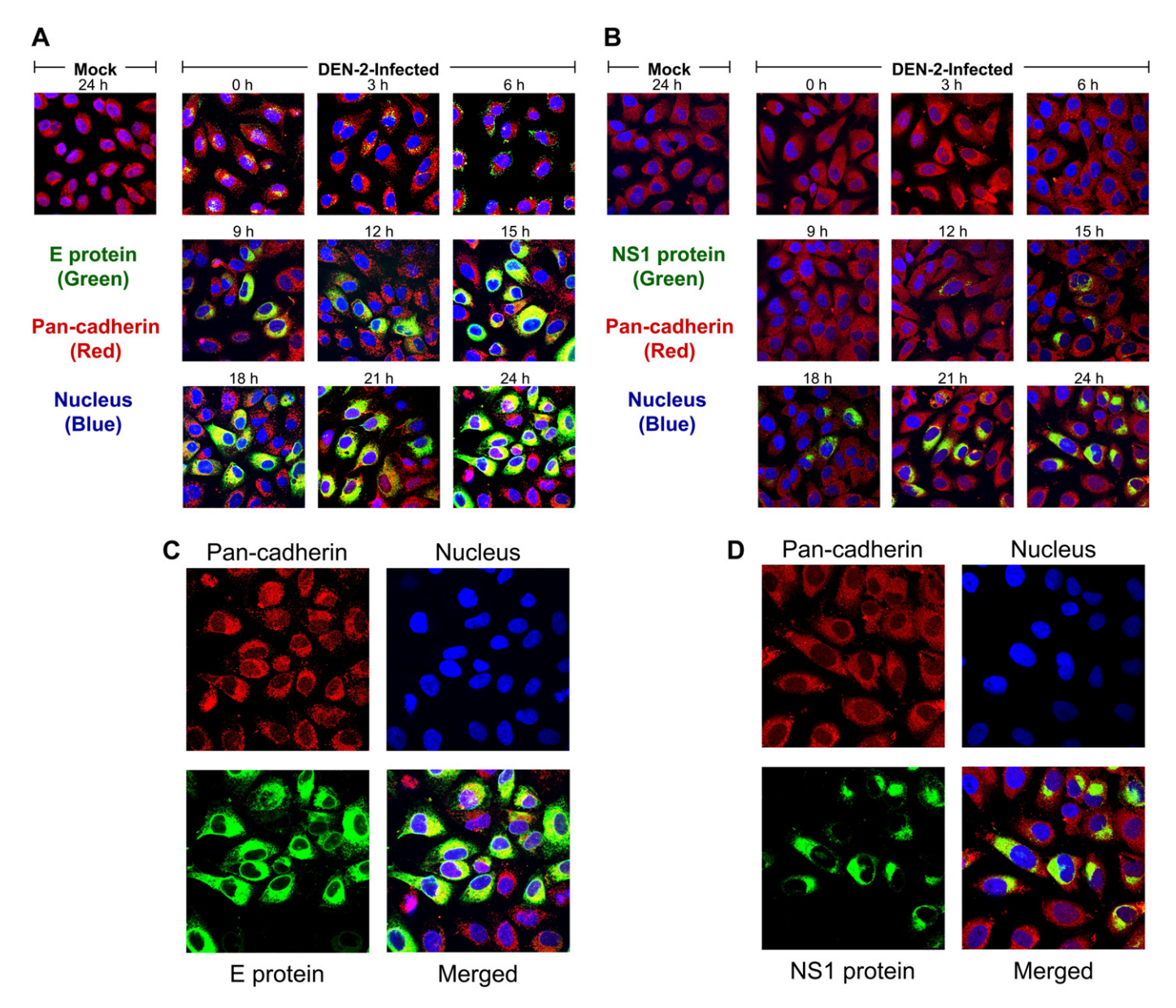


Fig. 3. Time-course double-immunofluorescence staining of dengue proteins (in green) and host pan-cadherin (in red), which is a marker for membrane/organelle. The nucleus was stained by Hoechst dye and is illustrated in blue. Expression of E and NS1 proteins was monitored for up to 24 h after the challenge with DEN-2 (at MOI 10 for 2 h) (panels (A) and (B), respectively). Co-localization of dengue proteins and pan-cadherin is illustrated as yellow. Panels (C) and (D) highlight the co-localization of pan-cadherin with E and NS1 proteins, respectively, at 24-h post-infection (the condition of which was used for Western blot analysis) to confirm the Western blot data presented in Fig. 2. Images were taken by a laser-scanning confocal microscope equipped with LSM5 Image Browser (LSM 510 Meta, Carl Zeiss; Jena, Germany). Original magnification power was 630X for all panels. (For interpretation of the references to colour in this figure legend, the reader is referred to the web version of this article.)

compartments. Briefly, the cells or their remaining compartments of cells were washed with PBS, fixed with 3.7% formaldehyde in PBS for 10 min, permeabilized by 1% triton X-100 in PBS for 10 min, followed by blocking with 1% bovine serum albumin (BSA) in PBS at room temperature (RT) for 1 h. After washing with PBS three times, they were initially incubated at 4 °C overnight with one of the following primary antibodies: rabbit polyclonal anti-calpain (marker for cytosol), mouse monoclonal anti-pan-cadherin (marker for membrane/organelle), mouse monoclonal anti-c-jun (marker for nucleus), and mouse monoclonal anti-pan-cytokeratin (marker for cytoskeleton) (all were purchased from Santa Cruz Biotechnology; Santa Cruz, CA; and all were diluted 1:200 in PBS). After washing with PBS, the cells or their remaining compartments were further incubated with donkey anti-rabbit or goat anti-mouse IgG conjugated with Cy3 (both were purchased from Jackson Immunoresearch Laboratories,

Inc.; West Grove, PA, and were diluted 1:10000 in PBS) at RT for 1 h. Images were taken by using a laser-scanning confocal microscope equipped with LSM5 Image Browser (LSM 510 Meta, Carl Zeiss; Jena, Germany).

3.4. Western blot analysis of dengue E and NS1 proteins in individual subcellular fractions

Proteins solubilized in these four fractions were precipitated with ProteoExtract Protein Precipitation Kit (Calbiochem, EMD Biosciences) for concentrating proteins and removal of interfering substances. Protein concentrations were determined by Bio-Rad protein assay (Bio-Rad Laboratories; Hercules, CA) based on Bradford's method [19]. Whole cell lysates derived from mock-control and DEN-2-infected EA.hy926 cells served as negative and

positive controls, respectively. Totally 20 µg equally loaded proteins derived from individual subcellular fractions (finally in a buffer containing 50 mM Tris—HCl pH 6.8, 2% SDS, 10% glycerol, and bromophenol blue; without dithiothreitol and mercaptoethanol) were resolved by unheated non-reducing SDS-PAGE (12% acrylamide). The resolved proteins were then transferred onto a nitrocellulose membrane and reacted with mouse monoclonal antibody against dengue E (clone 3H5) or NS1 (clone DN1) (Abcam; Cambridge, UK) (1:200 in 5% skim milk/PBS) at 4 °C overnight, and then with rabbit anti-mouse IgG conjugated with horseradish peroxidase (Santa Cruz Biotechnology; Santa Cruz, CA) (1:1000 in 5% skim milk/PBS) at RT for 1 h. Protein bands were visualized by SuperSignal West Pico chemiluminescence substrate (Pierce Biotechnology, Inc., Rockford, IL) and autoradiograph.

3.5. Time-course study of expression of dengue E and NS1 proteins, and their localization in membrane/organelle compartment

After the challenge with DEN-2 (at the MOI of 10 for 2 h), their expression was monitored for further 0-24 h. Mock EA.hy926 cells cultured in parallel to DEN-2-infected cells (but without DEN-2 infection) served as the negative control. The cell monolayers were washed with PBS, fixed with 3.7% formaldehyde in PBS for 10 min, permeabilized by 1% triton X-100 in PBS for 10 min, followed by blocking with 1% BSA/PBS at RT for 1 h. After washing with PBS three times, they were initially incubated at 4 °C overnight with goat polyclonal anti-pan-cadherin (Santa Cruz Biotechnology) (1:200 in PBS) together with mouse monoclonal antibody against dengue E protein (clone 3H5) or mouse monoclonal anti-NS1 (clone DN1) (Abcam) (1:50 in PBS). Thereafter, all the samples were washed and further incubated at RT for 1 h with donkey anti-goat IgG conjugated with phycoerythrin (Santa Cruz Biotechnology) (1:400 in PBS) together with goat anti-mouse IgG conjugated with Alexa 488 (Invitrogen-Molecular Probes; Eugene, OR) (1:2500 in PBS) and Hoechst dye (Invitrogen-Molecular Probes) (1:1000 in PBS for nuclear stain). Images were then captured using a laserscanning confocal microscope equipped with LSM5 Image Browser (LSM 510 Meta, Carl Zeiss).

Acknowledgements

We are grateful to Dr. Chunya Puttikhunt for providing cultured supernatant collected from hybridoma clone. This work was supported by the National Center for Genetic Engineering and Biotechnology (BIOTEC) (to SP and VT), Office of the Higher Education Commission and Mahidol University under the National Research Universities Initiative (to VT), and The Thailand Research Fund (RTA5380005) (to VT). JP was supported by Siriraj Graduate

Thesis Scholarship, whereas both SC and VT are also supported by "Chalermphrakiat" Grant, Faculty of Medicine Siriraj Hospital.

Appendix. Supplementary material

Supplementary data related to this article can be found online at doi:10.1016/j.micpath.2011.04.011.

References

- [1] Halstead SB. Dengue. Lancet 2007;370:1644-52.
- [2] Mukhopadhyay S, Kuhn RJ, Rossmann MG. A structural perspective of the flavivirus life cycle. Nat Rev Microbiol 2005;3:13–22.
- [3] Anderson R, King AD, Innis BL. Correlation of E protein binding with cell susceptibility to dengue 4 virus infection. J Gen Virol 1992;73(Pt 8):2155-9.
- [4] Bressanelli S, Stiasny K, Allison SL, Stura EA, Duquerroy S, Lescar J, et al. Structure of a flavivirus envelope glycoprotein in its low-pH-induced membrane fusion conformation. EMBO J 2004;23:728–38.
- [5] Perera R, Kuhn RJ. Structural proteomics of dengue virus. Curr Opin Microbiol 2008;11:369–77.
- [6] Hiscox JA. The interaction of animal cytoplasmic RNA viruses with the nucleus to facilitate replication. Virus Res 2003;95:13–22.
- [7] Weidman MK, Sharma R, Raychaudhuri S, Kundu P, Tsai W, Dasgupta A. The interaction of cytoplasmic RNA viruses with the nucleus. Virus Res 2003;95: 75–85.
- [8] Uchil PD, Kumar AV, Satchidanandam V. Nuclear localization of flavivirus RNA synthesis in infected cells. J Virol 2006;80:5451–64.
- [9] Kanlaya R, Pattanakitsakul SN, Sinchaikul S, Chen ST, Thongboonkerd V. Alterations in actin cytoskeletal assembly and junctional protein complexes in human endothelial cells induced by dengue virus infection and mimicry of leukocyte transendothelial migration. | Proteome Res 2009;8:2551–62.
- [10] Salonen A, Ahola T, Kaariainen L. Viral RNA replication in association with cellular membranes. Curr Top Microbiol Immunol 2005;285:139–73.
- [11] Lindenbach BD, Rice CM. Molecular biology of flaviviruses. Adv Virus Res 2003;59:23—61.
- [12] Winkler G, Maxwell SE, Ruemmler C, Stollar V. Newly synthesized dengue-2 virus nonstructural protein NS1 is a soluble protein but becomes partially hydrophobic and membrane-associated after dimerization. Virology 1989; 171:302-5
- [13] Winkler G, Randolph VB, Cleaves GR, Ryan TE, Stollar V. Evidence that the mature form of the flavivirus nonstructural protein NS1 is a dimer. Virology 1988:162:187–96.
- [14] Falgout B, Markoff L. Evidence that flavivirus NS1-NS2A cleavage is mediated by a membrane-bound host protease in the endoplasmic reticulum. J Virol 1995;69:7232—43.
- [15] Noisakran S, Sengsai S, Thongboonkerd V, Kanlaya R, Sinchaikul S, Chen ST, et al. Identification of human hnRNP C1/C2 as a dengue virus NS1-interacting protein. Biochem Biophys Res Commun 2008;372:67–72.
- [16] Kanlaya R, Pattanakitsakul SN, Sinchaikul S, Chen ST, Thongboonkerd V. Vimentin interacts with heterogeneous nuclear ribonucleoproteins and dengue nonstructural protein 1 and is important for viral replication and release. Mol Biosyst 2010;6:795–806.
- [17] Kim JH, Hahm B, Kim YK, Choi M, Jang SK. Protein-protein interaction among hnRNPs shuttling between nucleus and cytoplasm. J Mol Biol 2000;298: 395–405.
- [18] Pinol-Roma S, Dreyfuss G. Shuttling of pre-mRNA binding proteins between nucleus and cytoplasm. Nature 1992;355:730–2.
- [19] Bradford MM. A rapid and sensitive method for the quantitation of microgram quantities of protein utilizing the principle of protein-dye binding. Anal Biochem 1976;72:248–54.

Molecular BioSystems



Cite this: Mol. BioSyst., 2011, 7, 1917–1925

www.rsc.org/molecularbiosystems

PAPER

Calcium oxalate dihydrate crystal induced changes in glycoproteome of distal renal tubular epithelial cells†

Wararat Chiangjong, ^a Supachok Sinchaikul, ^b Shui-Tein Chen ^{bc} and Visith Thongboonkerd $*^{ad}$

Received 8th February 2011, Accepted 23rd March 2011 DOI: 10.1039/c1mb05052d

Calcium oxalate dihydrate (COD) crystals can adhere onto the apical surface of renal tubular epithelial cells. This process is associated with crystal growth and aggregation, resulting in kidney stone formation. Glycoproteins have been thought to play roles in response to crystal adhesion. However, components of the glycoproteome that are involved in this cellular response remain largely unknown. Our present study therefore aimed to identify altered glycoproteins upon COD crystal adhesion onto tubular epithelial cells representing distal nephron, the initiating site of kidney stone formation. Madin-Darby Canine Kidney (MDCK) cells were maintained in culture medium with or without COD crystals for 48 h (n = 5 flasks per group). Cellular proteins were extracted, resolved by 2-DE and visualized by SYPRO Ruby total protein stain, whereas glycoproteins were detected by Pro-Q Emerald glycoprotein dye. Spot matching and quantitative intensity analysis revealed 16 differentially expressed glycoprotein spots, whose corresponding total protein levels were not changed by COD crystal adhesion. These altered glycoproteins were successfully identified by O-TOF MS and/or MS/MS analyses, and potential glycosylation sites were identified by the GlycoMod tool. For example, glycoforms of three proteasome subunits (which have a major role in regulating cell-cell dissociation) were up-regulated, whereas a glycoform of actin-related protein 3 (ARP3) (which plays an important role in cellular integrity) was down-regulated. These coordinated changes implicate that COD crystal adhesion induced cell dissociation and declined cellular integrity in the distal nephron. Our findings provide some novel insights into the pathogenic mechanisms of kidney stone disease at the molecular level, particularly cell-crystal interactions.

Introduction

Kidney stones are mostly composed of calcium oxalate (CaOx) and are frequently associated with underlying metabolic disorders; *e.g.* hypercalciuria, hyperoxaluria and hypocitraturia. ¹ CaOx stone formation generally begins with nucleation, growth and aggregation of CaOx crystals. In addition to these pathogenic mechanisms, the other critical step is adhesion of CaOx crystals onto renal tubular epithelial cells. ² In human urine, CaOx crystals are predominately in dihydrate form

(COD), which can nucleate and adhere directly onto the apical surface of living renal tubular epithelial cells *via* the (100) face under appropriate conditions (*i.e.* decreased levels of inhibitors or, on the other hand, increased levels of promoters).^{3,4} The plasma membrane will promote their adhesion due to the nature of crystal-binding sites on the apical surface of the cells.^{5,6} The data obtained from previous studies indicate that COD-containing stone is commonly found in patients with high urinary calcium excretion.^{7,8}

Although COD crystals are frequently found in human urine and involved in kidney stone formation, a number of macromolecules; *i.e.* urinary glycoproteins (including Tamm–Horsfall protein, bikunin, nephrocalcin, and urinary prothrombin fragment I) can counterbalance the formation of kidney stone by their properties to inhibit crystal growth, aggregation and/or adhesion to renal tubular epithelial cells.^{1,9} Deficiency of these inhibitory glycoproteins in the urine has been proposed to enhance the stone formation.

At the apical surface of renal tubular epithelial cells, glycoproteins may aggravate crystal adhesion onto the plasma membrane. However, components of such surface

^a Medical Proteomics Unit, Office for Research and Development, Faculty of Medicine Siriraj Hospital, Mahidol University, 12th Fl. Adulyadej Vikrom Bldg., 2 Prannok Rd., Bangkoknoi, Bangkok 10700, Thailand. E-mail: thongboonkerd@dr.com, vthongbo@yahoo.com; Fax: +66-2-4184793; Tel: +66-2-4184793

^b Institute of Biological Chemistry and Genomic Research Center, Academia Sinica, Taipei, Taiwan

^c Institute of Biochemical Sciences, College of Life Science, National Taiwan University, Taipei, Taiwan

^d Center for Research in Complex Systems Science, Mahidol University, Bangkok, Thailand

[†] Electronic supplementary information (ESI) available. See DOI: 10.1039/c1mb05052d

glycoproteins are under investigation. Inside renal tubular epithelial cells, glycoproteins play diverse biological functions; e.g. cell-cell communications, cellular response and activation, etc. However, their role in crystal modulation and processing remains largely unknown. We therefore conducted the present study to explore altered cellular glycoproteome in renal tubular cells derived from distal nephron, the initiating site of kidney stone formation.

Results and discussion

Exposure to 100 μg mL⁻¹ COD crystals for 48 h caused adhesion of COD crystals onto MDCK cells, whereas cell death (apoptosis and necrosis) was not changed significantly (these data have been reported in our previous study). 10 Therefore, this treatment condition was suitable for the investigation of early response in MDCK cells during COD crystal adhesion. In the present study, we visualized glycoprotein spots resolved in 2-D gels using a fluorescent hydrazide Pro-Q Emerald 300 dye (Invitrogen-Molecular Probes). In principle, glycols in glycoproteins are oxidized to aldehydes using periodic acid, followed by conjugation with the fluorescent dye, which reacts with aldehyde groups. 11 The efficiency and specificity of Pro-Q Emerald 300 glycoprotein dye for staining carbohydrate residues are satisfactory and have been well addressed in several previous studies. 11 SYPRO Ruby (Invitrogen-Molecular Probes), a bathophenanthroline complex of ruthenium(II) that can interact with cationic amino acid residues on proteins, 12 was used for detection of total proteins within the same gel following the staining by Pro-Q Emerald 300 dye. The total protein staining by SYPRO Ruby on-top of glycoprotein staining by Pro-Q Emerald 300 had no interference because they were detectable by different excitation wavelengths (532 nm for SYPRO Ruby, but 300 nm for Pro-Q Emerald 300). This allowed precise matching of glycoprotein spots to their corresponding total protein spots. With an equal amount (200 µg) of total proteins equally loaded into each gel, 235 \pm 22 glycoprotein spots were detected by Pro-Q Emerald 300 dye, whereas 850 ± 19 total protein spots were detected by staining with SYPRO Ruby dye. This result indicated that the high proportion of total proteins were glycosylated, consistent with the data reported previously. 13

After spot matching using a 2-D gel image analysis software (Image Master 2D Platinum), quantitative intensity analysis revealed significantly altered levels of 16 glycoprotein spots (8 were increased in COD-treated cells, 5 were decreased in COD-treated cells, 2 were present only in COD-treated cells, and 1 was absent after COD adhesion), whose corresponding total protein levels did not change significantly (Fig. 1). These altered glycoproteins were then identified by Q-TOF MS and/or MS/MS analyses. Their identities, quantities and related data are summarized in Table 1, whereas their respective protein levels determined by SYPRO Ruby are shown in Table S1 (ESI†). While our previous study reported changes in levels of some proteins, 10 the present study demonstrated changes in glycosylation status or altered levels of glycoforms of identified proteins, not their total protein levels. As the goal and design of these two studies differed (particularly, changes

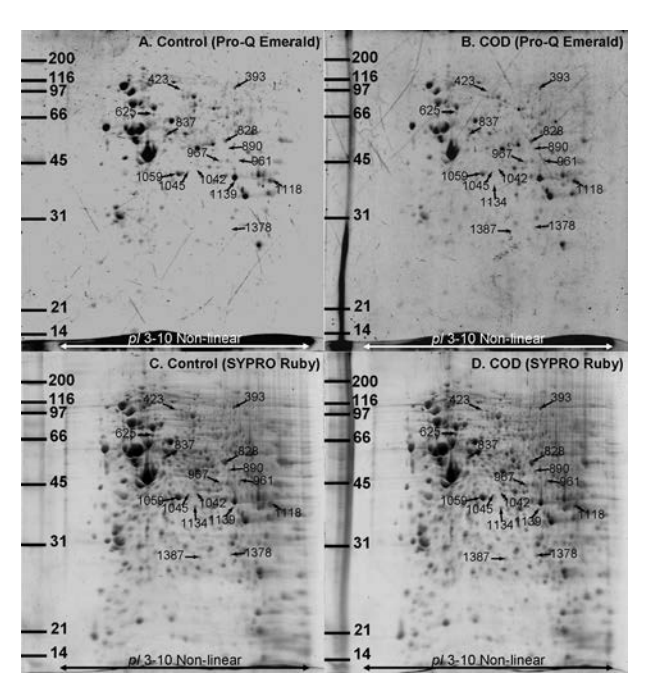


Fig. 1 2-D map of altered glycoproteome in MDCK cells in response to COD crystal adhesion. Proteins derived from whole cell lysate of MDCK cells cultured in the absence (A and C) or presence (B and D) of COD crystals were resolved by 2-DE (non-linear pH gradient of 3–10). The resolved glycoprotein spots were visualized with Pro-Q Emerald 300 glycoprotein stain (A and B). Thereafter, the glycoproteins-stained gels were stained with SYPRO Ruby total protein dye to visualize total protein spots (C and D) (n = 5 gels derived from individual cultured flasks for each set; 200 µg equally loaded into each gel). Significantly differed glycoprotein spots, whose corresponding total protein spots had no significant changes (labeled with numbers in this map), were identified by Q-TOF MS and/or MS/MS analyses (Table 1).

in total protein levels were excluded from the present study), there were no common changes found in these two studies.

The altered glycoproteins in MDCK tubular cells in response to COD crystal adhesion identified in the present study were related to or involved in many biological processes as summarized in Table 2. Using the GlycoMod tool, many potential *N*-linked glycosylation sites were identified in the altered glycoproteins (Table 3; see also Table S2, ESI†). Potential roles of these glycoproteins in renal tubular epithelial cells in response to COD crystal adhesion are emphasized as follows.

We found increased levels of glycoforms of three unique proteins (one glycoform was increased, whereas the other two glycoforms were observed only in the COD-treated cells), which belong to the proteasome family and have a major role in regulating cell–cell dissociation during cell movement. We also observed decreased level of a glycoform of actin-related protein 3 (ARP3), which plays an important role in cellular integrity. These data implicate that COD crystal adhesion might induce cell dissociation and decline cellular integrity in renal tubular epithelial cells of the distal nephron.

Interestingly, we identified a macrophage scavenger receptor in MDCK cells and its glycoform was increased in the COD-treated cells. In macrophage, it is a membrane glycoprotein

Table 1 Summary of glycoproteins whose levels of glycoforms, not their total protein levels, were significantly altered in MDCK cells during COD crystal adhesion

				Identification	%Cov ^b	No. of matched	_		Intensity by Pro-Q Emerald dye (Mean \pm SEM)	l i	Ratio	
Spotnc	Spot no. Protein name	$NCBI^a$ ID	Identified by	(MS, MS/MS)		(MS, MS/MS)	Id	MW/kDa	Control	COD-treated (Control)	p values
Glycopr 303	Glycoproteins whose levels of glycoforms were significantly increased	significantly incre		in COD-treated MDCK cells	ells	13 NA	72.9	85 87	0.0870 + 0.0540	0.2731 ± 0.0561	3 11	5700
423	Cytokeratin type II	gi 73996498	MS/MS	NA, 52	2/, NA NA, 1	NA, 1	6.33	107.86	$0.05/9 \pm 0.0340$ 0.0704 ± 0.0311	0.2731 ± 0.0201 0.1784 ± 0.0266	2.54	0.030
068	Macrophage scavenger receptor	gi 293746	MS	73, NA	27, NA	10, NA	89.9	50.18	0.0104 ± 0.0104		14.32	0.022
961	type 1 Translocase of outer mitochondrial	gi 73947367	MS, MS/MS	58, 65	23, 5	5, 1	8.24	32.59	0.0132 ± 0.0132	0.2655 ± 0.0568 2	20.11	0.003
	membrane 40 homolog isoform 2						0	0	-		!	0
967 1042	PIBF1 protein Isocitrate dehydrogenase 3 (NAD+)	gi 116283307) gi 73951310	MS MS, MS/MS	72, NA 142, 143	31, NA 45, 14	10, NA 12, 4	6.03 5.86	49.82 35.09	0.0399 ± 0.0246 0.0070 ± 0.0070	0.1902 ± 0.0560 0.1547 ± 0.0465 2	4.77 22.06	0.039 0.014
	alpha isoform 2					;			-		0	6
1045	Protein phosphatase 1, catalytic submit alpha	gi 50978728	MS	98, NA	43, NA	11, NA	5.94	38.13	0.0132 ± 0.0132	0.0925 ± 0.0245	6.99	0.022
1378	Proteasome subunit beta type 3	gi 57091113	MS	119, NA	58, NA	12, NA	6.15	23.25	0.0538 ± 0.0330	0.2769 ± 0.0275	5.15	0.001
	(proteasome theta chain) (proteasome chain 13)											
	(proteasome component C10-II)											
Glycopr 625	Glycoproteins whose levels of glycoforms were significantly decreased 625 Heteropeneous puclear ribonucleo- oil 55958547 MS	significantly decr	eased in COD-tr MS MS/MS	in COD-treated MDCK cells MS/MS 122 42 38	ells 38-2	12.1	5 43	42.01	0.3117 ± 0.0601	0.0549 ± 0.0341	0 18	900 0
ì	protein K		2	î	i	î	;	i				
828	Alpha enolase (2-phospho-D-glyce-	gi 73956716	MS/MS	NA, 196	NA, 15	NA, 4	6.57	45.47	0.4358 ± 0.0495	0.2689 ± 0.0323	0.62	0.022
	rate hydro-lyase) (non-neural en- olase) (NNE) (enolase 1)											
	(phosphopyruvate hydratase) (C-myc	၁										
	promoter-binding protein) (MBP-1)											
	(plasminogen-binding protein)											
	isoform 1											
837	ARP3 actin-related protein 3	gi 73984196	MS, MS/MS	105, 99	26, 6	12, 3	6.87	64.27	0.4068 ± 0.1093	0.1321 ± 0.0417	0.32	0.047
1059	Annexin A1 (annexin I) (lipocortin I) gi/73946797) gi 73946797	MS, MS/MS	146, 238	48, 12	14, 3	5.84	38.89	0.6623 ± 0.0752	0.4305 ± 0.0399	0.65	0.026
	(calpactin II) (chromobindin 9) (P35)											
1118	(phosphonpase A2 innibitory protein) Heterogeneous muclear ribonucleo-	u) oi!73976124	SM/SM SM	170 146	57 15	15.3	8 74	22 62	0 9071 + 0 0476	0.6283 ± 0.0779	69 0	0.016
0111	protein A2/B1 isoform 2	61/2//2/18		, , ,	, , ,	,,		1		10.0	6	0.00
Glycopr	Glycoproteins whose glycoforms were present only in COD-treated M	nly in COD-trea	ted MDCK cells									
1134	Proteasome (prosome, macropain)	gi 74004396	MS	76, NA	46, NA	8, NA	00.9	33.48	0.0000 ± 0.0000	$0.0733 \pm 0.0235 \text{ #DIV/0}$		0.014
	26S subunit, non-ATPase, 14 isoform 2											
1387	Proteasome (prosome, macropain)	gi 109114737	MS, MS/MS	68, 66	37, 8	7, 1	6.15	22.90	0.0000 ± 0.0000	$0.2225 \pm 0.0645 ~ \sharp$	#DIV/0	0.009
Chiann	subunit, beta type, 3 isoform 1	M Possous a O										
013copn 1139	Orycoproteins whose grycoforms were absent in COD-treated at D.C.A. 1139 Annexin A2 gi 50950177 MS,	gi 50950177	MS, MS/MS	191, 141	51, 12	15, 3	6.92	38.92	0.3483 ± 0.0970	$0.3483 \pm 0.0970 \ \ 0.0000 \pm 0.0000 \ \ 0.00$	00.0	0.007
$N_{\mathbf{A}}$	$NA = not \text{ applicable}; \#DIV/0 = divided by zero^a NCBI = National Center for Biotechnology Information; ^b %Cov$	$zero^a NCBI =$	National Cente	r for Biotechno	logy Informat	\parallel	%sedne	ice covera	ge [(number of th	%sequence coverage [(number of the matched residues/total number of	/total nu	ımber of
residue	residues in the entire sequence) \times 100%].											

Table 2 Subcellular localization, molecular function and biological process of the identified proteins^a

Spot no.	Protein name	Subcellular localization	Molecular function	Biological process
Glycopro	oteins whose levels of glycoforms were sign	ificantly increased in COD-tre	eated MDCK cells	
393	Elongation factor 2 (EF-2)	Cytoplasm	Elongation factor	Protein biosynthesis
423	Cytokeratin type II	Intermediate filament	Structural molecule activity	Cytoskeleton organization
890	Macrophage scavenger receptor type I	Membrane; single-pass type II membrane protein		Endocytosis
961	Translocase of outer mitochondrial membrane 40 homolog isoform 2	Mitochondrion outer membrane; multi-pass membrane protein	Porin	Ion and protein transport
967	PIBF1 protein	NA	Mediator of progesterone	NA
1042	Isocitrate dehydrogenase 3 (NAD+) alpha isoform 2	Mitochondria	Oxidoreductase	Tricarboxylic acid cycle
1045	Protein phosphatase 1, catalytic subunit, alpha	Cytoplasm	Hydrolase, protein phosphatase	Carbohydrate and glycogen metabolism, cell cycle/division
1378	Proteasome subunit beta type 3 (proteasome theta chain) (proteasome chain 13) (proteasome component C10-II)	Cytoplasm, nucleus	Hydrolase, protease, threonine protease	Anaphase-promoting complex- dependent proteasomal ubiquitin- dependent protein catabolic process/mitotic cell cycle
Glycopro	oteins whose levels of glycoforms were sign	ificantly decreased in COD-tre		
625	Heterogeneous nuclear ribonucleoprotein K	Cytoplasm, nucleus	Ribonucleoprotein	mRNA processing/splicing
828	Alpha enolase (2-phospho-D-glycerate hydro-lyase) (non-neural enolase) (NNE) (enolase 1) (phosphopyruvate hydratase) (C-myc promoter-binding protein) (MBP-1) (MPB-1) (plasminogen-binding protein) isoform 1	Cytoplasm, nucleus, cell membrane	Lyase/repressor	Glycolysis, plasminogen activity, translation, translation regulation
837	ARP3 actin-related protein 3 homolog	Cytoplasm	ATP/actin binding	Regulation of actin filament polymerization
1059	Annexin A1 (annexin I) (lipocortin I) (calpactin II) (chromobindin 9) (P35) (phospholipase A2 inhibitory protein)	Nucleus, cytoplasm, basolateral membrane	Phospholipase A2 inhibitor	Anti-apoptosis, cell motion, inflammatory response, cell surface receptor linked signal transduction, calcium ion binding
1118	Heterogeneous nuclear ribonucleoprotein A2/B1 isoform 2	Cytoplasm, nucleus	Ribonucleoprotein	mRNA processing/splicing
Glycopro	otein's whose glycoforms were present only	in COD-treated MDCK cells		
1384	Proteasome (prosome, macropain) 26S subunit, non-ATPase, 14 isoform 2		Hydrolase, protease, threonine protease	Anaphase-promoting complex- dependent proteasomal ubiquitin- dependent protein catabolic process/mitotic cell cycle
1387	Proteasome (prosome, macropain) subunit, beta type, 3 isoform 1	Cytoplasm, nucleus	Hydrolase, protease, threonine protease	Anaphase-promoting complex- dependent proteasomal ubiquitin- dependent protein catabolic process/mitotic cell cycle
Glycopro 1139	oteins whose glycoforms were absent in CO Annexin A2	D-treated MDCK cells Extracellular matrix, secreted, basement membrane	Calcium ion binding	Calcium-regulated membrane-bindin protein, skeleton system developmen

^a Obtained from the UnitProt Protein Knowledgeable Database; NA = not applicable.

with an implicated role in the pathologic deposition of low density lipoproteins (LDL) in arterial wall during atherogenesis. Moreover, Type I subunit of this glycoprotein acts as a receptor to mediate endocytosis of a diverse group of macromolecules, including acetylated LDL. In renal tubular cells, its precise role remains unknown but can be postulated to be associated with COD crystal adhesion and internalization into the adherent cells. ^{2,17}

In metabolic pathways, we identified increased glycoforms of isocitrate dehydrogenase 3 (NAD+) alpha isoform 2 (IDH3 α) and protein phosphatase 1 catalytic subunit alpha (PP1 α) in the COD-treated cells. These enzymes are generally involved in catalytic activity especially in glycolysis. IDH3 α , as a catalytic enzyme belonging to the IDH family, plays a crucial role in oxidative decarboxylation of isocitrate to

generate ATP in the tricarboxylic acid cycle, which is regulated by numerous allosteric regulators. 18,19 In addition, the IDH activity is activated by a calcium ion in the presence of isocitrate and adenine nucleotide. 18 PP1 α regulates a variety of cellular processes, including carbohydrate and glycogen metabolism, cell division, and protein synthesis. Furthermore, it is required for dephosphorylation of partitioning-defective (Par)-3, which is localized at the apical junctional complex and is essential for formation of an apical–basal polarity and tight junction. 20,21 We hypothesized that the altered levels of their glycoforms were related to altered metabolisms in renal tubular epithelial cells in response to COD crystal adhesion.

Heterogeneous nuclear ribonucleoproteins (hnRNPs) are the major nucleic acid-binding proteins involving in gene expression processes; i.e. transcriptional regulation, alternative pre-mRNA splicing and processing. We observed changes in glycoforms of hnRNP K and hnRNP A2/B1

induced by COD crystal adhesion. hnRNP K has multiple functions, including pre-mRNA processing and mRNA export from nucleus, and acts as a versatile DNA-RNA binding

Table 3 Potential *N*-linked glycosylation sites identified by the "GlycoMod" tool (peptides containing the motif "N–X–S/T/C" where X was not P)^a

Snot No	Protein name	Residues	Saguanca	Number of peptide masses identified		
			Sequence		glycosylation	
393	Elongation factor 2 (EF-2)	1–10	MV <u>N</u> F <u>T</u> VDQIR	2	1221.62 1237.61	17 13
		1–15	MV <u>NFT</u> VDQIRAIMDK	3	1779.90 1795.90 1811.89	1 4 2
		17–32	ANIR NM SVIAHVDHGK	2	1760.91 1776.91	6 4
		21–32	<u>NMS</u> VIAHVDHGK	2	1306.65 1322.64	12 9
		21-42	NMSVIAHVDHGKSTLTDSLV CK	4		0
		608–641	GHVFEESQVAGTPMFVVKAY LPVNESFGFTADLR	2	_	0
		626-641	AYLPVNESFGFTADLR	1	1798.89	3
		626–679	AYLPVNESFGFTADLRSNTG GQAFPQCVFDHWQILPGDPF DNTSRPSQVVAETR	4	_	0
		642–679	SNTGGQAFPQCVFDHWQILP GDPFDNTSRPSQVVAETR	4	_	0
		642–680	SNTGGQAFPQCVFDHWQILP GDPFD NT SRPSQVVAETRK	4	_	0
423	Cytokeratin type II	82–144	SGFGGRASGGFGAGSGFGYG GAAGGGYGAWGFPVCPPGGI QEVTVNQSLLTPLNLQIDPA IQR	4	_	0
		88–144	ASGGFGÄGSGFGYGGAAGGG YGAWGFPVCPPGGIQEVTVN QSLLTPLNLQIDPAIQR	4	_	0
		88–146	ASGGFGAGSGFGYGGAAGGG YGAWGFPVCPPGGIQEVTV <u>N</u>	4	_	0
		286–324	QSLLTPLNLQIDPAIQRVR MLFEAELSQMQTQVSDTSVV LSMDN <u>NRS</u> LDLDSIIAEVK	4	_	0
		325-335	AQYEDIA NRS R	1	1321.64	8
		454–486	LLEGEECRLSGEGVSPVNIS IQNSSVSVSQGGK	2	_	0
		462-486	LSGEGVSPVNISIQNSSVSV SQGGK	1	_	0
		462–499	LSGEGVSPV <u>NIS</u> IQNSSVSV SQGGKSFGGSFGGGFGTR	1	_	0
		521–582	ASSGGAGYGLGLGGMGYRAG GAFGGYGFGGGMMSGSAGIQ EVTVNQSLLTPLHLEIDPSL QR	4	_	0
		539-582	AGGAFGGYGFGGGMMSGSAG IQEVTVNQSLLTPLHLEIDP SLQR	3	_	0
		539–584	AGGAFGĞYGFGGGMMSGSAG IQEVTVNQŞLLTPLHLEIDP SLQRVR	3	_	0
		761–771	AQYEDIA NRS R	1	1321.64	8
		890–951	LLEGEECRLTGEGVGPV <u>NIS</u> VVSSSGGTGYSSGGGSLCMT GGGYSSSLGYSSGGGFSSTS GR	6	_	0
		898–951	LTGEGVGPV <u>NIS</u> VVSSSGGT GYSSGGGSLCMTGGGYSSSL	4	_	0
		898–961	GYSSGGGFSSTSGR LTGEGVGPV <u>NIS</u> VVSSSGGT GYSSGGGSLCMTGGGYSSSL	8	_	0
		952–961	GYSSGGGFSSTSGR <u>NMS</u> GSS SSMR NMSGSSSSMR	3	1042.42	3
		752 701	CODDOMIK	J	1058.41	5
					1074.41	3
		952-965	<u>NM</u> SGSSSSMRIISK	3	1483.71	4
					1499.71 1515.70	3 2
625	Heterogeneous nuclear	67–86	ALRTDYNASVSVPDSSGPER	1	_	0
	ribonucleoprotein K	70–86	TDYNASVSVPDSSGPER	1	_	0
		70–102	TDY <u>NAS</u> VSVPDSSGPERILS ISADIETIGEILK	1		0

Table 3 (continued)

Alpha enolase (2-phospho-bg/gyterute hydro-lysus)	ked Number of on glycoforms		Number of peptide masses identified	Sequence	Residues	Protein name	Spot No.
Con-neural enolase) (NNE) 1510.70 1526.7	3 9						828
Cenolase 1) (phosphopyruate hydratase) (C-my promoter) inding protein) (MBP-1) (plansinogen-binding protein) isoform 1 1-9	9		3	LIMENIDO I EI NES K	93-103	(non-neural enolase) (NNE) (enolase 1) (phosphopyruvate hydratase) (C-myc promoter-	
hydrataso C-myc promoter-binding protein MBP-1)	8						
MPB-1) (plasminogen-binding protein) soform 1							
1-19							
ARP3 actin-related protein 1-26 MVEPESLNQTIEESHPDOK 2							
Nomolog	0	_	2	MVEPESI NOTIFESHPDOK	1-19		837
type I	0	_			1-26	homolog	
90-110 NTSDTSÖGPMEKENTSNVEM R 3 102-110 ENTSNVEMR 2 1078.47 1094.47	1					1 6 6 1	890
102-110 ENTSNVEMR 2 1078.47 1094.57 1094.47 1094.47 1094.47 1094.47 1094.47 1094.57 1094.47 1094.47 1094.47 1094.57 1094.47 1094.47 1094.57 1094.47	1					type I	
102-119 ENTSNVEMRFTIIMAHMK 4 2199.01 133-151 ADLIDTGRFQNFSMATDQR 2 1343.59 141-151 FQNFSMATDQR 2 1343.59 141-178 FQNFSMATDQRLNDILLQLN 2	2						
133-151 ADLIDTGREQNESMATDQR 2 1343.59 1345.69 1345.69	2		-	E. Igi (E. III)	102 110		
141-151	2	2199.01			102-119		
141-178	0						
141-178	1 1		2	FQNESMATDQR	141–151		
152-200	0	1339.39 —	2	FONESMATDORLNDILLOLN	141-178		
179-200 SLQSLNMTLLDVQ	Ů		-		1.11 1.70		
LHTETLHVR	0	_	2		152-200		
179-200 SLQSLNMTLLDVQLHTETLH VR 2							
179-202 SLÓSLMTLLDVÓLHTETLH VRVR 2	0		2		170 200		
242-255 QEVRVLNNITNDLR	0	_					
PIBF1 protein	9	1682.91					
PIBF1 protein 11-40 EVALUATION EVALU	18						
1	15						
108-139 17 108-139 17 17 17 17 17 17 17 1	0 5						
961 Translocase of outer mitochondrial membrane 40 homolog isoform 2 103–139 LTVNKGLSNHFQVNHTVALS TVGES TVGESNYHFGVTYVGTK 1 — 967 PIBF1 protein 11–40 KVNISSSLESEDISLETTVP TDDISSSEER 1 — 12–40 VNISSSLESEDISLETTVPT DDISSSEER 1 — 12–43 VNISSSLESEDISLETTVPT DDISSSEER 1 — 12–243 VNISSSLESEDISLETTVPT DDISSSEER 1 — 12–249 VNISSSLESEDISLETTVPT DDISSSEEREGK 1 — 231–239 NYSEVQIR 1 1007.50 232–239 NYSEVQIR 1 1007.50 232–242 NYSEVQIRCQR 2 1394.67 1451.69 388–400 TNQEIDQLRNASR 1 1543.77 397–400 NASR 1 146.22 397–405 NASREMYER 2 1170.51	9			`			
40 homolog isoform 2 108-139 GLSNHFQVNHTVALSTVGES NYHFGVTYYGTK 108-173 GLSNHFQVTYVGTK 108-173 GLSNHFQVTYVGTKQLSPTEAF PVLVGDMDNSGSLNAQVIHQ LGPGLR 11-40 KVNISSSLESEDISLETTVP 1	Ó	_				Translocase of outer	961
NYHFGVTYVGTK							
108-173 GLSNHFQVNHTVALSTVGES 2	0	_	1		108–139	40 homolog isoform 2	
NYHFGVTYVGTKQLSPTEAF	0	_	2		108-173		
PVLVGDMDNSGSLNAQVIHQ LGPGLR	V		-	·	100 175		
967 PIBF1 protein 11-40 KVNISSSLESEDISLETTVPT TDDISSSEER 1 — 12-40 VNISSSLESEDISLETTVPT DDISSSEER 1 — 12-43 VNISSSLESEDISLETTVPT DDISSSEERGK 1 — 231-239 KNYSEVQIR 1 1007.50 232-239 NYSEVQIR 1 1007.50 232-242 NYSEVQIRCQR 2 1394.67 1451.69 388-400 TNQEIDQLRNASR 1 1543.77 397-400 NASR 1 446.22 397-405 NASREMYER 2 1154.51 1042 Isocitrate dehydrogenase 3 (NAD+) alpha isoform 2 9-27 APIQWEERNYTAIQGPGGK 2 — 1042 Isocitrate dehydrogenase 3 (NAD+) alpha isoform 2 17-27 NYTAIQGPGGK 1 1040.56 17-35 NYTAIQGPGGKWMIPPEAK 4 —				· · · · · · · · · · · · · · · · · · ·			
12-40 VNISSSLESEDISLETTVPT 1							
12-40	0	_	1		11–40	PIBF1 protein	967
12-43 VNISSSEER 12-43 VNISSSLESEDISLETTVPT 1	0	_	1		12-40		
DDISSSEEREGK 231–239 KNYSEVQIR 1 1135.60 232–239 NYSEVQIR 1 1007.50 232–242 NYSEVQIR 2 1394.67 1451.69 388–400 TNQEIDQLRNASR 1 1543.77 397–400 NASR 1 446.22 397–405 NASREMYER 2 1154.51 1170.51 1170.51 1042 Isocitrate dehydrogenase 3 9–27 APIQWEERNYTAIQGPGGK 2	V		1		12 40		
231-239 KNYSEVQIR 1 1135.60 232-239 NYSEVQIR 1 1007.50 232-242 NYSEVQIR 2 1394.67 1451.69 388-400 TNQEIDQLRNASR 1 1543.77 397-400 NASR 1 446.22 397-405 NASREMYER 2 1154.51 1170.51 1170.51 1042 Isocitrate dehydrogenase 3 9-27 APIQWEERNYTAIQGPGGK 2	0	_	1	V <u>NIS</u> SSLESEDISLETTVPT	12-43		
232-239	1.7	1125.60			221 220		
232-242 NYSEVQIRCQR 2 1394.67 1451.69 388-400 TNQEIDQLRNASR 1 1543.77 397-400 NASR 1 446.22 397-405 NASREMYER 2 1154.51 1170.51 1042 Isocitrate dehydrogenase 3 (NAD+) alpha isoform 2 17-27 NYTAIQGPGGK 1 1040.56 17-35 NYTAIQGPGGKWMIPPEAK 4	17 16			*			
1451.69 388-400 TNQEIDQLRNASR 1 1543.77 397-400 NASR 1 446.22 397-405 NASREMYER 2 1154.51 1042 Isocitrate dehydrogenase 3 9-27 APIQWEERNYTAIQGPGGK 2	13						
397-400 NASR 1 446.22 397-405 NASREMYER 2 1154.51 1170.5	7		_				
1042 Isocitrate dehydrogenase 3 9-27 APIQWEERNYTAIQGPGGK 2 1154.51 1170.51 1040.56 17-35 NYTAIQGPGGKWMIPPEAK 4	5						
1170.51 1042 Isocitrate dehydrogenase 3 9–27 APIQWEERNYTAIQGPGGK 2 — (NAD+) alpha isoform 2 17–27 NYTAIQGPGGK 1 1040.56 17–35 NYTAIQGPGGKWMIPPEAK 4 —	19						
1042 Isocitrate dehydrogenase 3 9–27 APIQWEERNYTAIQGPGGK 2 — (NAD+) alpha isoform 2 17–27 NYTAIQGPGGK 1 1040.56 17–35 NYTAIQGPGGKWMIPPEAK 4 —	5 4		2	NASKEWYEK	397-403		
(NAD+) alpha isoform 2 17–27 NYT AIQGPGGK 1 1040.56 17–35 NYT AIQGPGGKWMIPPEAK 4 —	0		2	APIOWEERNVTAIOGPGGK	9–27	Isocitrate dehydrogenase 3	1042
	5	1040.56					1042
130 150 NINIADENIATA VIII 1 1775 71	0						
- 	15	1375.71	1	NNHRSNYTAVHK SNVTAVHK	139–150		
143–150 SNYTAVHK 1 854.46 143–155 SNYTAVHKANIMR 2 1439.77	18 22						
145 155 SIVIAVIIKAIVIIK 2 1455.76	19		-		110 100		
Protein phosphatase 1, 261–301 RQLVTLFSAPNYCGEFDNAG 12 —	0	_	12		261-301		1045
catalytic subunit, alpha AMMSVDETLMCSFQILKPAD K	0		10		262 221	catalytic subunit, alpha	
262–301 QLVTLFSAP <u>N</u> YCGEFDNAGA 12 — MMSVDETI MCSEQU V BADV	0	_	12		262–301		
MMSVDETLMCSFQILKPADK 262–303 QLVTLFSAP NY CGEFDNAGA 12 —	0	_	12		262-303		
MMSVDETLMCSFQILKPADK NK	U		12		202 303		

Table 3 (continued)

Spot No.	Protein name	Residues	Sequence	Number of peptide masses identified	Peptide mass with <i>N</i> -linked glycosylation	
1059	Annexin A1 (annexin I) (lipocortin I) (calpactin II) (chromobindin 9) (P35) (phospholipase A2 inhibitory protein)	None of the (X not P)'	he peptides obtained by cleavage of protein .	sequence contains	s the motif 'N-	X-S/T/C
1118	Heterogeneous nuclear ribo- nucleoprotein A2/B1 isoform 2 isoform 22	None of the (X not P)'	he peptides obtained by cleavage of protein .	sequence contains	s the motif 'N-	X-S/T/C
1134	Proteasome (prosome,	224-246	SWMEGLTLQDYSEHCKHNES VVK	8	_	0
	macropain) 26S subunit,	240-246	HNESVVK	1	811.42	20
	non-ATPase, 14 isoform 2	240-253	HNESVVKEMLELAK	2	1625.85	9
					1641.84	12
1139	Annexin A2	50-68	GVDEVTIVNILT NRS NEQR	1	2156.12	2
1378	Proteasome subunit beta type 3 (Proteasome theta chain) (Proteasome chain 13) (Proteasome component C10-II)	(X not P)'	he peptides obtained by cleavage of protein	sequence contains	s the motif 'N-	X-S/T/C
1387	Proteasome (prosome, macropain) subunit, beta type, 3 isoform 1		he peptides obtained by cleavage of protein	sequence contains	s the motif 'N-	X-S/T/C
^a More de	etails can be found in ESI.†					

protein and/or a scaffold protein integrating in signal transduction pathways.^{22,23} It is found in nucleus, cytoplasm and mitochondria, and also plays a role in maintaining the cellular ATP level under stress conditions through protection of target mRNAs.^{22,24} hnRNP A2/B1 is widely distributed, particularly near nucleoli, and has a well-presented role in RNA processing, especially splicing.^{25,26} Moreover, it has a potential role in cell growth but, on the other hand, promotes cell death in transformed and cancer cells.^{26,27} However, the mechanistic insights of declined levels of hnRNPs' glycoforms in renal tubular epithelial cells upon COD crystal adhesion remain unknown and should be further investigated.

In summary, we identified altered levels of glycoforms of 16 proteins in MDCK renal tubular epithelial cells in response to COD crystal adhesion. These proteins generally play important roles in many cellular functions. Changes in their glycoforms might be associated with alterations in cellular integrity and metabolisms, as well as COD crystal adhesion and internalization. These findings may provide some novel insights into the pathogenic mechanisms of kidney stone disease.

Materials and methods

Preparation of COD crystals

COD crystals were generated as we previously described. Die Briefly, 125 mL of 25.08 mM CaCl₂·2H₂O was added into 250 mL of a solution containing 19.26 mM C₆H₅Na₃O₇·2H₂O, 23.1 mM MgSO₄·7H₂O and 127.4 mM KCl. When the solution was homogeneously mixed, the pH of the solution was adjusted to 6.5 using HCl and then incubated at 25 °C for 15 min. Thereafter, 125 mL of 6.4 mM Na₂C₂O₄ was added into the solution under continuous stirring and further incubated at 25 °C for 15 min. COD crystals were separated from the solution after centrifugation at 2000 × g for 5 min. The supernatant was discarded and the crystals were resuspended

in absolute methanol. After centrifugation at $2000 \times g$ for 5 min, methanol was discarded, whereas the crystals were air-dried at 25 °C overnight. The presence and purity of COD crystals were confirmed by phase-contrast microscopy.

Cell culture

Madin-Darby Canine Kidney (MDCK) cells, which were derived from dog kidney and exhibited distal renal tubule phenotype, 28 were used as a model of mammalian cells derived from distal nephron. Approximately 3×10^6 MDCK cells were cultured in each 75 cm² tissue culture flask containing a complete Eagle's minimum essential medium (MEM) (GIBCO, Invitrogen Corporation; Grand Island, NY) supplemented with 10% fetal bovine serum, 1.2% penicillinG/streptomycin, and 2 mM glutamine. The cultured cells were maintained in a humidified incubator at 37 °C with 5% CO₂ for 24 h.

COD crystal adhesion

A total of 10 semi-confluent flasks were then divided into two sets (n=5 each), and the cultured medium was replaced by either COD crystal-containing or crystal-free medium. For the COD crystal-containing medium, after COD crystal generation and harvest, the crystals were decontaminated by UV irradiation for 30 min and then added to MEM to the final concentration of 100 μ g of COD crystals per 1 mL of medium. For the crystal-free medium, COD crystals with an equal amount of 100 μ g mL⁻¹ were added into the medium for 30 min but then removed from the medium to make the identical concentrations of free calcium and oxalate ions in the medium compared to the COD crystal-containing medium. The cells were further maintained for 48 h.

Protein extraction

After cultivation of MDCK cells with or without COD crystals for 48 h, the cells were harvested by scraping, then

removed into the tube containing 0.5 M EDTA in PBS and further incubated at 4 °C for 30 min to dissolve the adherent COD crystals. Thereafter, the cells were washed with PBS three times to remove EDTA, then resuspended in a lysis buffer (7 M urea, 2 M thiourea, 4% 3-[(3-cholamidopropyl) dimethyl-ammonio]-1-propanesulfonate (CHAPS), 120 mM dithiothreitol (DTT), 2% ampholytes (pH 3–10), and 40 mM Tris-HCl), and incubated at 4 °C for 30 min. The suspensions were then centrifuged at $9100 \times g$ to remove unsolubilized debris and particulate matter. Protein concentrations were measured by the Bradford assay.

Two-dimensional gel electrophoresis (2-DE)

An equal amount of 200 µg of proteins derived from each sample was mixed with a rehydration buffer (7 M urea, 2 M thiourea, 2% CHAPS, 120 mM DTT, 40 mM Tris-base, 2% ampholytes (pH 3-10), and a trace amount of bromophenol blue) to make the final volume of 150 µL per sample. The samples were then rehydrated onto individual Immobiline DryStrip (nonlinear pH gradient of 3-10, 7 cm long; GE Healthcare, Uppsala, Sweden) at room temperature for 16 h. The isoelectric focusing (IEF) was performed in an Ettan IPGphor III IEF System (GE Healthcare) at 20 °C using a stepwise mode to reach 9083 V h. After the completion of IEF, the strips were equilibrated in an equilibration buffer (6 M urea, 130 mM DTT, 112 mM Tris-base, 4% SDS, 30% glycerol, and 0.002% bromophenol blue) for 15 min at room temperature and then incubated with a similar buffer (where 130 mM DTT was replaced with 135 mM iodoacetamide) for 15 min at room temperature. The proteins on the equilibrated strips were further separated on 13% polyacrylamide gel using a SE260 mini-Vertical Electrophoresis Unit (GE Healthcare) at 150 V for approximately 2 h.

Glycoprotein staining

Glycoproteins separated on 2-D gels were visualized with Pro-Q Emerald 300 glycoprotein gel stain (Invitrogen-Molecular Probes; Eugene, OR). Briefly, the gels were fixed in a fixing solution (50% methanol and 5% acetic acid) for 45 min twice and then washed with 3% glacial acetic acid for 10-20 min twice. The carbohydrates on the gels were oxidized by oxidizing solution (1% (w/v) periodic acid diluted with 3% acetic acid) for 30 min and then washed with 3% glacial acetic acid for 10-20 min three times. Thereafter, the gels were stained with fresh Pro-Q Emerald 300 staining solution (diluting the Pro-Q Emerald 300 stock solution 50-fold into Pro-Q Emerald 300 staining buffer) for 90 min in the dark and then washed with 3% glacial acetic acid for 15-20 min twice. All steps were performed at room temperature with gentle agitation. The gels were scanned using a 300 nm UV transilluminator (the GeneGenius Gel Imaging System-Syngene; Frederick, MD).

Total protein staining

The glycoprotein-stained gels were stained again with SYPRO Ruby total protein gel stain (Invitrogen-Molecular Probes). Briefly, the gels were fixed in a fixing solution (10% methanol and 7% acetic acid) for 30 min and then stained with SYPRO Ruby dye overnight in the dark. After staining, the gels were

destained in a destaining solution (10% methanol and 7% acetic acid) for 30 min followed by washing in deionized water for 5 min three times. The gels were scanned using a Typhoon laser scanner (GE Healthcare). Gel images were captured with an excitation of 532 nm and emission of 610 nm band-pass filter. The photo-multiplier tube (PMT) was tuned to 600 V to obtain the resolution at 100 µm pixel size, which produced 100 data points per cm and 200 data lines per grid square.

Matching and analysis of glycoprotein and protein spots

The glycoprotein and total protein spots were detected and matched by Image Master 2D Platinum (GE Healthcare) software. Parameters used for spot detection were (i) minimal area = 10 pixels; (ii) smooth factor = 2.0; and (iii) saliency = 2.0. A reference gel was created as a collection of all gel images. The reference gel was used for matching the glycoprotein and protein spots among gels. Background of each gel was subtracted and the intensity volume of each spot was normalized with the total intensity volume from all spots on individual gels.

Statistical analysis

Intensity levels of individual corresponding (matched) spots across gels were compared between the two sets of the MDCK cells (control vs. COD-treated) using unpaired Student's *t*-test. *P*-Values less than 0.05 were considered statistically significant. Only significantly differed glycoprotein spots (stained by Pro-Q Emerald), whose corresponding total protein spots (stained by SYPRO Ruby) had no significant changes, were subjected to in-gel tryptic digestion and identification by quadrupole time-of-flight (Q-TOF) mass spectrometry (MS) and tandem MS (MS/MS).

In-gel tryptic digestion

The differentially expressed glycoprotein spots were excised from 2-D gels, washed twice with 200 µl of 50% acetonitrile (ACN)/25 mM NH₄HCO₃ buffer (pH 8.0) at room temperature for 15 min, and then washed once with 200 µL of 100% ACN. After washing, the solvent was removed and the gel pieces were dried by a SpeedVac concentrator (Savant; Holbrook, NY). The dried gel plugs were then rehydrated with 10 µL of 1% (w/v) trypsin (Promega; Madison, WI) in 25 mM NH₄HCO₃. After rehydration, the gel pieces were crushed with a siliconized blue stick and incubated at 37 °C for at least 16 h. Peptides were subsequently extracted twice with 50 μL of 50% ACN/5% trifluoroacetic acid (TFA); the extracted solutions were then combined and dried with the SpeedVac concentrator. The peptide pellets were resuspended with 10 μL of 0.1% TFA and purified using ZipTip_{C18} (Millipore). The peptide solution was drawn up and down in the ZipTip_{C18} 10 times and then washed with 10 µL of 0.1% formic acid by drawing up and expelling the washing solution three times. The peptides were finally eluted with 5 µL of 75% ACN/0.1% formic acid.

Mass spectrometry (Q-TOF MS and/or MS/MS) and sequence analyses

The trypsinized samples were premixed 1:1 with the matrix solution containing 5 mg mL $^{-1}$ α -cyano-4-hydroxycinnamic

acid (CHCA) in 50% ACN, 0.1% (v/v) TFA and 2% (w/v) ammonium citrate, and deposited onto the 96-well MALDI target plate. The samples were analyzed by a Q-TOF UltimaTM mass spectrometer (Micromass; Manchester, UK), which was fully automated with a predefined probe motion pattern and the peak intensity threshold for switching over from MS survey scanning to MS/MS, and from one MS/MS to another. Within each sample well, parent ions that met the predefined criteria (any peak within the m/z 800–3000 range with intensity above 10 count ± include/exclude list) were selected for CID MS/MS using argon as the collision gas and a mass dependent \pm 5 V rolling collision energy until the end of the probe pattern was reached. The MS and MS/MS data were extracted and output as the searchable .txt and .pkl files, respectively, for independent searches using the MASCOT search engine (http://www.matrixscience.com), assuming that peptides were monoisotopic. Fixed modification was carbamidomethylation at cysteine residues, whereas variable modification was oxidation at methionine residues. Only one missed trypsin cleavage was allowed, and peptide mass tolerances of 100 and 50 ppm were allowed for peptide mass fingerprinting and MS/MS ions search, respectively. Thereafter, sequences of the identified proteins were subjected to analyses for their potential functions reported in the UniProt Protein Knowledgeable Database (http://www.uniprot.org) as well as for their potential N-linked glycosylation sites using the GlycoMod tool (http://www.expasy.ch/tools/glycomod/).

Abbreviations

2-DE two-dimensional gel electrophoresis

ACN acetonitrile

ARP actin-related protein

CHAPS 3-[(3-cholamidopropyl) dimethyl-ammonio]-1-

propanesulfonate

cyano-4-hydroxycinnamic acid CHCA COD calcium oxalate dihydrate

DTT dithiothreitol

N,N,N',N'-ethylenediaminetetraacetic acid **EDTA ERK** extracellular signal-regulated kinase heterogeneous nuclear ribonucleoprotein hnRNP

IDH isocitrate dehydrogenase **IEF** isoelectric focusing

MDCK Madin-Darby Canine Kidney **MEM** minimum essential medium

MS mass spectrometry Par partitioning-defective

PIBF progesterone-induced blocking factor

PMF peptide mass fingerprinting PP1α protein phosphatase 1 alpha

TFA trifluoroacetic acid

Acknowledgements

We are grateful to Tistaya Semangoen and Sakdithep Chaiyarit for their technical assistance. We also thank the Core Facilities for Proteomics and Structural Biology Research, Institute of Biological Chemistry, Academia Sinica,

Taiwan. This study was supported by Office of the Higher Education Commission and Mahidol University under the National Research Universities Initiative, and The Thailand Research Fund (RTA5380005) (to V. Thongboonkerd). V. Thongboonkerd is also supported by "Chalermphrakiat" Grant, Faculty of Medicine Siriraj Hospital, whereas W. Chiangjong is supported by the Royal Golden Jubilee PhD Program of The Thailand Research Fund.

References

- 1 M. S. Parmar, BMJ [Br. Med. J.], 2004, 328, 1420-1424.
- 2 J. C. Lieske and S. Deganello, J. Am. Soc. Nephrol., 1999, 10(suppl 14), S422-S429.
- 3 J. C. Lieske, F. G. Toback and S. Deganello, Kidney Int., 2001, 60, 1784-1791
- 4 X. Sheng, M. D. Ward and J. A. Wesson, J. Am. Soc. Nephrol., 2005, 16, 1904-1908.
- 5 J. C. Lieske, F. G. Toback and S. Deganello, Kidney Int., 1998, 54, 796-803
- 6 J. C. Lieske, F. G. Toback and S. Deganello, Calcif. Tissue Int., 1996, 58, 195-200.
- 7 B. T. Murphy and L. N. Pyrah, Br. J. Urol., 1962, 34, 129-159.
- 8 A. Trinchieri, C. Castelnuovo, R. Lizzano and G. Zanetti, Urol. Res., 2005, 33, 194-198.
- 9 E. M. Worcester, Semin. Nephrol., 1996, 16, 474-486.
- 10 T. Semangoen, S. Sinchaikul, S. T. Chen and V. Thongboonkerd, J. Proteome Res., 2008, 7, 2889-2896.
- 11 T. H. Steinberg, K. Pretty On Top, K. N. Berggren, C. Kemper, L. Jones, Z. Diwu, R. P. Haugland and W. F. Patton, *Proteomics*, 2001. 1. 841–855.
- 12 T. H. Steinberg, E. Chernokalskaya, K. Berggren, M. F. Lopez, Z. Diwu, R. P. Haugland and W. F. Patton, Electrophoresis, 2000, 21. 486-496.
- 13 O. Vagin, J. A. Kraut and G. Sachs, Am. J. Physiol. Renal Physiol., 2009, 296, F459-F469.
- 14 T. Tsukamoto and S. K. Nigam, J. Biol. Chem., 1999, 274, 24579-24584.
- 15 P. Dalhaimer, T. D. Pollard and B. J. Nolen, J. Mol. Biol., 2008, **376**, 166–183.
- 16 A. Matsumoto, M. Naito, H. Itakura, S. Ikemoto, H. Asaoka, I. Hayakawa, H. Kanamori, H. Aburatani, F. Takaku and H. Suzuki, Proc. Natl. Acad. Sci. U. S. A., 1990, 87, 9133-9137.
- 17 M. S. Schepers, R. A. Duim, M. Asselman, J. C. Romijn, F. H. Schroder and C. F. Verkoelen, Kidney Int., 2003, 64, 493-500
- 18 Y. O. Kim, H. J. Koh, S. H. Kim, S. H. Jo, J. W. Huh, K. S. Jeong, I. J. Lee, B. J. Song and T. L. Huh, J. Biol. Chem., 1999, 274,
- 19 D. T. Hartong, M. Dange, T. L. McGee, E. L. Berson, T. P. Dryja and R. F. Colman, Nat. Genet., 2008, 40, 1230-1234.
- 20 X. Chen and I. G. Macara, Nat. Cell Biol., 2005, 7, 262-269.
- 21 T. Hirose, Y. Izumi, Y. Nagashima, Y. Tamai-Nagai, H. Kurihara, T. Sakai, Y. Suzuki, T. Yamanaka, A. Suzuki, K. Mizuno and S. Ohno, J. Cell Sci., 2002, 115, 2485-2495.
- 22 K. Bomsztyk, O. Denisenko and J. Ostrowski, Bioessays, 2004, 26, 629-638
- 23 G. Dreyfuss, V. N. Kim and N. Kataoka, Nat. Rev. Mol. Cell Biol., 2002, 3, 195-205.
- 24 T. Fukuda, T. Naiki, M. Saito and K. Irie, Genes Cells, 2009, 14, 113-128.
- 25 L. R. Friend, S. P. Han, J. A. Rothnagel and R. Smith, Biochim. Biophys. Acta, 2008, 1783, 1972-1980.
- 26 A. Mayeda, S. H. Munroe, J. F. Caceres and A. R. Krainer, EMBO J., 1994, 13, 5483-5495.
- 27 C. Patry, L. Bouchard, P. Labrecque, D. Gendron, B. Lemieux, J. Toutant, E. Lapointe, R. Wellinger and B. Chabot, Cancer Res., 2003, 63, 7679–7688.
- 28 M. H. Saier, Jr., Am. J. Physiol., 1981, 240, C106-C109.